

# Chapter 21

## Evaluation of Mass-Spring-Damper Models for Dynamic Interaction Between Walking Humans and Civil Structures

Ahmed S. Mohammed and Aleksandar Pavic

**Abstract** Dynamic interaction between walking humans and vibrating flexible structures is one of the main challenges when simulating human-induced vibrations. To account for this interaction, several mass-spring-damper (MSD) models featuring different parameters have recently been proposed. This paper compares the performance of six experimentally-based MSD models of walking humans available in the literature. The simulated vibration responses of these models were compared with experimental measurements of four human test subjects walking on a full-scale flexible footbridge. Numerical simulations were carried out for two cases: non-interactive and interactive models using the above mentioned MSD models. Moreover, for each case two models of walking forces were used: previously measured continuous walking forces (from a treadmill test) for the corresponding test subjects and a deterministic walking force function from design guidelines. It is demonstrated that neglecting human-structure interaction in the simulations can result in a significant overestimation of the vibration responses. By utilising any of the interactive models of walking people, the accuracy of the vibration response predictions can be improved. The best performance was obtained when both the measured walking forces and the interactive model were used.

**Keywords** Human-structure interaction • Human-induced vibrations • Walking forces • Mass-spring-damper • Footbridge

### 21.1 Introduction

The advancements of structural materials and design techniques have enabled engineers to design more slender and longer span civil structures such as footbridges, floors and grandstands. While the strength requirements are usually assured, the structural design of such structures has been increasingly governed by vibration serviceability criteria related to human dynamic excitation including walking and running [1].

There is a growing number of cases of structures which are either over- or under-designed for vibration serviceability according to current design methods. This indicates a lack of reliable methods for prediction and assessment of human-induced vibration [2]. For lightweight slender structures, one of the main challenges in developing such methods is the complexity of the dynamic interaction between walking people and their accommodating structure [3, 4]. To consider using this interaction in a design method, recently, there has been proliferation of walking-related human-structure interaction (HSI) models [5]. The performance of these models have not been compared with each other, and therefore, there is a need to evaluate their performance using experimental measurements.

This paper compares the performance of six experimentally-developed HSI models for walking humans [6–11]. Experimental measurements pertinent to four people walking on a full-scale slender footbridge were used for this purpose. Furthermore, two models of walking forces were utilised in the analysis: measured walking forces (from nominally identical treadmill walking test for corresponding test subjects) and the traditional walking force model based on Fourier series representation.

---

A.S. Mohammed (✉) • A. Pavic  
Vibration Engineering Section, College of Engineering, Mathematics and Physical Sciences,  
University of Exeter, Kay Building, North Park Road, Exeter, EX4 4QF, UK  
e-mail: [asm221@exeter.ac.uk](mailto:asm221@exeter.ac.uk)

## 21.2 Human-Structure Interaction Models of Walking Humans

The existence of walking people is proven to have an effect on the dynamic behaviour of their accommodating structure. This effect can be mainly observed as an increased modal damping and a change in natural frequency due to the coupling between the walking people and supporting structure during walking [1, 5, 12].

HSI models of walking humans can generally be divided into three groups according to their approaches: mass-spring-damper (MSD) models, inverted-pendulum models and more complex models of the human body. This paper considers only the first group, as it is the most widely used and user-friendly approach in the vibration serviceability community. It comprises either a single or multiple MSDs attached to the supporting structure, replicating the dynamic behaviour of a walking human, as shown in Fig. 21.1.

In this study, the performance of six experimentally-developed MSD models of a single person walking [6–11] were compared. These models represent nominally identical human walking and the only difference between them is the parameters of the mass, stiffness and damping. Table 21.1 presents MSD parameters of eight experimentally-developed models of HSI of walking humans available in the literature.

The model presented by Lou et al. [13] is excluded from the comparison, as the suggested range of natural frequency of the walking human is considerably below the range reported of other models. The model presented by Silva [14] is also excluded from the comparison. It was originally developed for crowds of walking people based a model of a single walking human [8]. These two models [8, 14] have relatively close MSD parameters so the model presented in [14] is excluded.

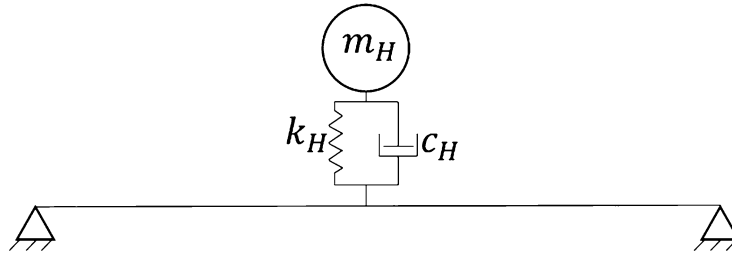


**Fig. 21.1** MSD representation of a walking human on a simply supported footbridge beam

**Table 21.1** Experimentally developed MSD parameters for walking human model available in the literature

No.	Study	Natural frequency ( $f$ ) (Hz)	Mass ( $m$ ) (kg)	Stiffness ( $k$ ) (N/m)	Damping	
					Damping coefficient ( $c$ ) (N s/m)	Damping ratio (%)
1	Jiménez-Alonso and Sáez [6]	2.75	84% of body mass ( $M$ )	–	–	47
2	Lou et al. [13]	1.25–1.60	100% of body mass ( $M$ )	–	–	37–50
3	Shahabpoor et al. [7]	2.75–3.0	100% of body mass ( $M$ )	–	–	27.5–30
4	Silva and Pimentel [8]	–	$97.082 + 0.275 M - 37.518 f_p$	$30351.744 - 50.26 c + 0.035 c^2$	$29.041 m^{0.883}$	–
5	Silva et al. [14]	–	$97.082 + 0.275 M - 37.518 f_p$	$5758.441 + 11.103 c$	$107.455 + 16.208 m$	–
6	Toso et al. [9]	–	<sup>a</sup>	<sup>b</sup>	<sup>c</sup>	–
7	Van Nimmen et al. [10]	2.5–4.0	95% of body mass	–	–	20–40
8	Zhang et al. [11]	1.85	100% of body mass	–	–	30

$$^a m = -231.34 + 3.69 M + 145.06 f_p - 1.97 M f_p + 0.005 M^2 - 15.25 f_p^2$$

$$^b k = 75601.45 - 1295.32 M - 33786.75 f_p + 506.44 M f_p + 3.59 M^2 + 539.39 f_p^2$$

$$^c c = -1115.69 + 92.56 M - 108.94 m + 2.91 M m - 1.33 M^2 - 1.30 m^2$$

## 21.3 Method

The performance of the six HSI models of walking people mentioned in Sect. 21.2 is evaluated by comparing the simulated vibration response using each model with their experimental counterpart of a human walking on a full-scale footbridge. The work explained in this study can be divided into three stages: identification of dynamic properties of the test structure, walking tests and simulations of vibration responses.

### 21.3.1 Test Structure

The walking tests were carried out on a laboratory footbridge located in the Structures Lab at the University of Exeter. The footbridge is 15 m long and 2.5 m wide. It consists of Sandwich Plate System (SPS) plates connected by thin plates and supported by perimeter steel beams using steel bolts.

A preliminary modal test was carried out to identify the modal properties of the test structure. The natural frequency and mode shapes of the first, second and third bending modes are presented in Fig. 21.2.

Since the natural frequency of the second vertical bending mode is much higher than the range of the fundamental natural frequency of walking human models (Table 21.1), only the fundamental mode of the test structure is considered in this study. Moreover, since the structure is flexible and can have relatively high vibration response due to human walking, it is expected that the nonlinear effects are not negligible. Therefore, the amplitude-dependent damping ratio and fundamental frequency were investigated. A series of tests by a single person bouncing on the middle on the structure were carried out to obtain the freely decaying response. For each test, the person was bouncing with the same frequency (controlled by a metronome) as the fundamental frequency of the footbridge (3.81 Hz) to achieve a resonant vibration response before jumping off the footbridge. In this way, the decaying response of the bare structure can be measured without interference from the excitation source, which was the bouncing person in this case. The decaying vibration response is considered from the moment the bouncing person jumps off the footbridge. To achieve this, two synchronised wireless Inertial Measurement Units (IMUs) were utilised, one was fixed on the leg of the person and the other one was fixed on the mid-span of the footbridge. In this way, it was possible to define the moment when the jumping person leaves the footbridge. A low-pass filter was then applied to the measured vibration responses, before the cycle by cycle fitting was used to determine the amplitude-dependent damping ratio and fundamental frequency, as shown in Fig. 21.3.

The modal mass was estimated from another test. A sinusoidal driving force was applied on the structure using a shaker at the same frequency as the frequency of the first bending mode (3.81 Hz). The driving force and the resulting vibration responses were measured during the test.

Numerical simulations of a single degree of freedom (SDOF) system representing the first bending mode were carried out. The identified amplitude-dependent natural frequency and damping ratio and the measured driving force of the shaker were utilised in these simulations. A range of modal masses were used and for each simulation the simulated and measured responses were compared. It was possible to identify the modal mass (5100 kg) by trial and error when the simulated response matches the measured response.

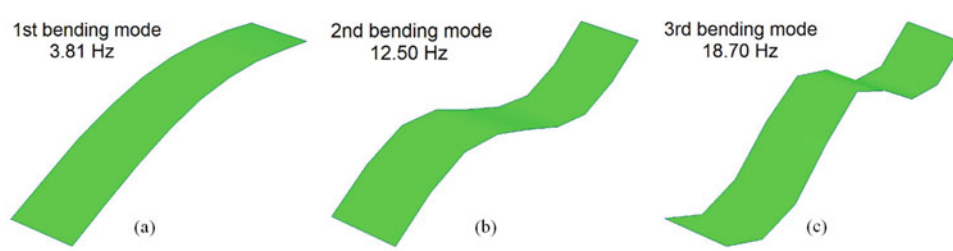


**Fig. 21.2** (a) First, (b) second and (c) third bending modes of the test structure

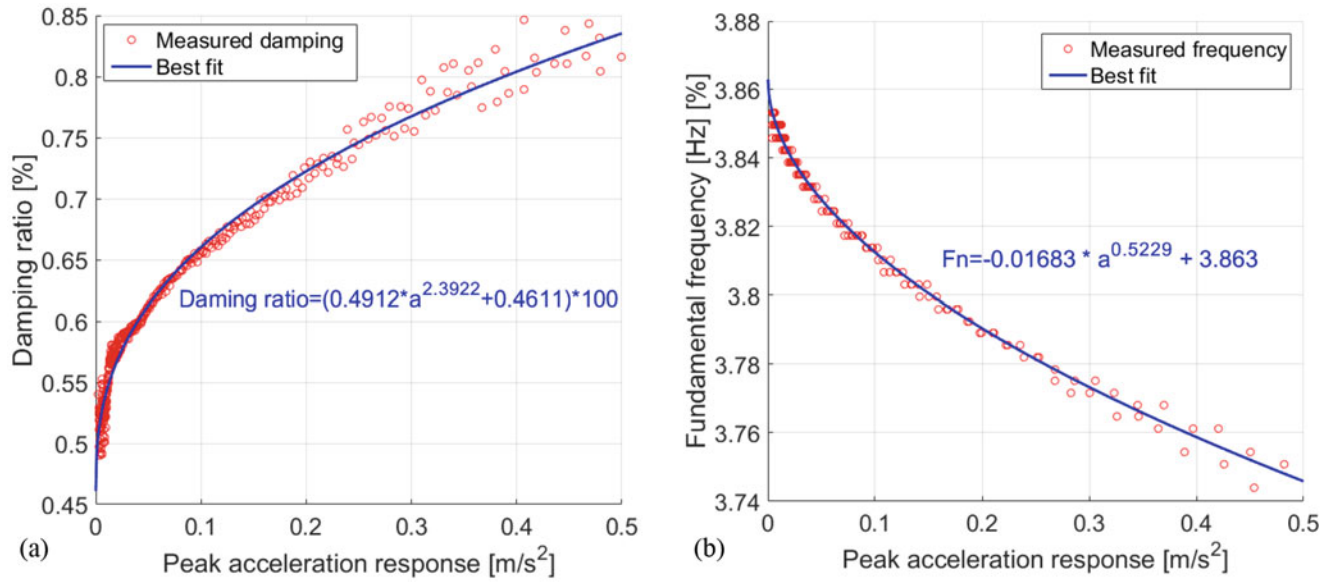


Fig. 21.3 Amplitude-dependent values of (a) damping ratio and (b) fundamental frequency of the test structure

### 21.3.2 Walking Tests

Walking tests were carried out individually by four male test subjects. Their weight range between 820 and 900 N and they were denoted as (TS1, TS2, TS3 and TS4). To take into account the intra-subject variability, each TS performed six walking tests at two pacing frequencies: 1.90 Hz and 2.05 Hz (12 walking tests in total). The second harmonic of the former pacing frequency excites the first bending mode of the footbridge and produces a resonant response. The later pacing frequency is chosen to obtain a non-resonant response. All walking tests were controlled by a metronome and each TS had to wait for about 10 s (at the location of one of the supports) between every two successive tests to allow for the vibration decay. The vibration response for each case was measured at the anti-node of the first vibration mode (mid-span of the footbridge).

### 21.3.3 Simulation of Vibration Responses

The identified dynamic properties of the first bending mode (Sect. 21.3.1) were utilised in the simulations of vibration responses. A MATLAB script was developed to take into account the amplitude-dependent damping ratio and fundamental frequency. The values of these parameters were updated after each cycle of the simulated vibration responses.

The simulations carried out in this study can be classified into two groups:

- Non-interactive models, for which HSI is neglected and only the walking force is applied on the oscillator of the vibration mode, and
- Interactive models, which include the HSI of walking people (as discussed in Sect. 21.2).

For each group, two types of walking forces are utilised:

- Measured walking forces for corresponding test subjects, and
- Deterministic walking force function based on Fourier series representation which can be mathematically described in Eq. (21.1):

$$F(t) = W \left( 1 + \sum_{n=1}^N \alpha_n \sin(2n\pi f_p t + \phi_n) \right), \quad (21.1)$$

where  $t$  is time (s),  $F(t)$  is the walking force (N),  $W$  is the static weight of the subject (kg),  $n$  is the harmonic number,  $N$  is the total number of harmonics,  $\alpha_n$  is the Fourier coefficient of the  $n$ th harmonic, which is also known as dynamic load factor (DLF),  $f_p$  is pacing frequency and  $\varphi_n$  is the phase shift of the  $n$ th harmonic.

Based on the above mentioned simulation groups, nine cases of simulations are considered in this study:

- Deterministic force and non-interactive model (DF-N).
- Measured force and non-interactive model (MF-N).
- Deterministic force and Silva's model [8] of walking people (DF-Si).
- Measured force and Alonso's model [6] of walking people (MF-A).
- Measured force and Shahabpoor's model [7] of walking people (MF-Sh).
- Measured force and Silva's model [8] of walking people (MF-Si).
- Measured force and Toso's model [9] of walking people (MF-T).
- Measured force and Van Nimmen's model [10] of walking people (MF-V).
- Measured force and Zhang's model [11] of walking people (MF-Z).

It is worth mentioning that the simulated vibration responses are repeated six times to replicate the experimentally measured vibration responses.

## 21.4 Results and Discussion

### 21.4.1 Results

In this section, the simulated vibration responses described in Sect. 21.3.3 are compared with their experimental counterparts. Two approaches are utilised for comparison, and as follows:

- Maximum 1-second Root Mean Square (RMS).
- Statistical comparison of vibration responses.

The process of comparing the simulations is schematically illustrated in Fig. 21.4 and the description of each procedure is presented in this section.

The maximum 1-second RMS is calculated for each measured and simulated vibration response. There are six walking tests/simulations for each case (i.e. six maximum 1-second RMS), and the average value is calculated and considered for comparison. This average value is normalised by its experimental counterpart and the results are presented in Fig. 21.5.

The maximum 1-second RMS does not provide a clear description of the overall vibration responses, as it is based on the maximum 1-second of the vibration response only. The cumulative distribution of the vibration responses can provide more informative description. Hence, it is used to compare the measured and simulated vibration responses. Figure 21.6 presents the cumulative distribution function (CDF) of the experimental and simulated vibration responses for a test subject at two pacing frequencies.

The concept of fractiles is utilised to compare the CDF of the measured and simulated vibration responses. In this study, a certain fractile of a vibration signal refers to the proportion of vibration signal with magnitude up to that value. The fractile related to any probability of non-exceedance (0–100%) can be extracted from the CDF plots. Figure 21.7 compares the fractiles of two simulations with their experimental counterparts. Interestingly, the fractiles of up to 90% probability of non-exceedance of all simulation cases follow almost a linear line which does not necessarily slope at 45° (Fig. 21.7). This means there is a trend of over- or under-estimation of vibration responses for vibration magnitudes with probability of non-exceedance up to 90%. Hence, the ratio of simulated/measured fractiles for this range is utilised to estimate the slope of the best linear line that passes through them (Fig. 21.7). This slope is the ratio of the vertical/horizontal components of the line. A slope of 1.1, for example, indicates an overestimation for vibration response for up to 90% of the vibration signal. This feature is used to compare the measured and simulated responses for all simulation cases, and the values of the slope for all simulation cases are presented in Table 21.2. The overall performance of each model is demonstrated by calculating the average absolute difference (from 1.0) of each fractile ratio as shown in the last row in Table 21.2.

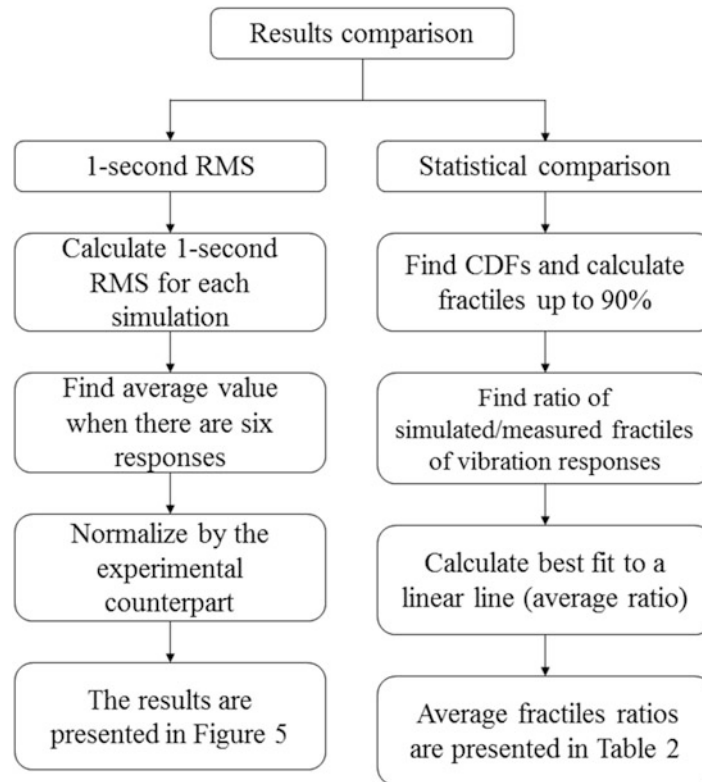


Fig. 21.4 Schematic overview of the results comparison approaches

### 21.4.2 Discussion

Section 21.4.1 provided comparison between the measured and simulated vibration responses in terms of vibration magnitudes up to 90% probability of non-exceedance and the maximum 1-second RMS. Hence, they can be used to describe the performance of the simulated models.

Simulated vibration responses for all non-interactive models are found to significantly overestimate the measured vibration responses in most of the cases, especially for the resonant responses (Fig. 21.5 and Table 21.2). Less conservative vibration responses are generally obtained when any of the interactive models are used. This is in line with previous findings that neglecting the interaction between walking people and the supporting structure can result in overestimation of vibration responses [4, 15]. Interestingly, none of the utilised HSI models of walking people performed particularly better than the others. However, the models presented by Silva [8] and Alonso [6] appear to perform slightly better than the others in most of the simulation cases (Fig. 21.5 and Table 21.2).

It is worth mentioning that the simulated vibration responses using any of the HSI models has less difference from the measured responses in the non-resonant cases (when pacing frequency is 2.05 Hz) than in the resonant case (1.90 Hz). This could indicate sensitivity to damping or amplitude-dependent parameters of the HSI models of walking humans. Another possible source of error is the variability of walking human model parameters between different people (inter-subject variability). This could be better addressed by repeating the test and simulations for a larger number of people.

The utilised measured walking forces model appears to have a non-negligible effect on the accuracy of the simulated vibration responses (Fig. 21.5 and Table 21.2). Therefore, despite the improved accuracy of the simulated responses, when any of the HSI models of walking humans is used, it can be even more improved when a more realistic walking forces model is used (the measured forces). This emphasises the importance of utilising a narrow-band near-periodic walking force model instead of the traditional periodic walking force model. Figure 21.8 shows an example of measured and simulated vibration responses when a measured force and an interactive model are used.

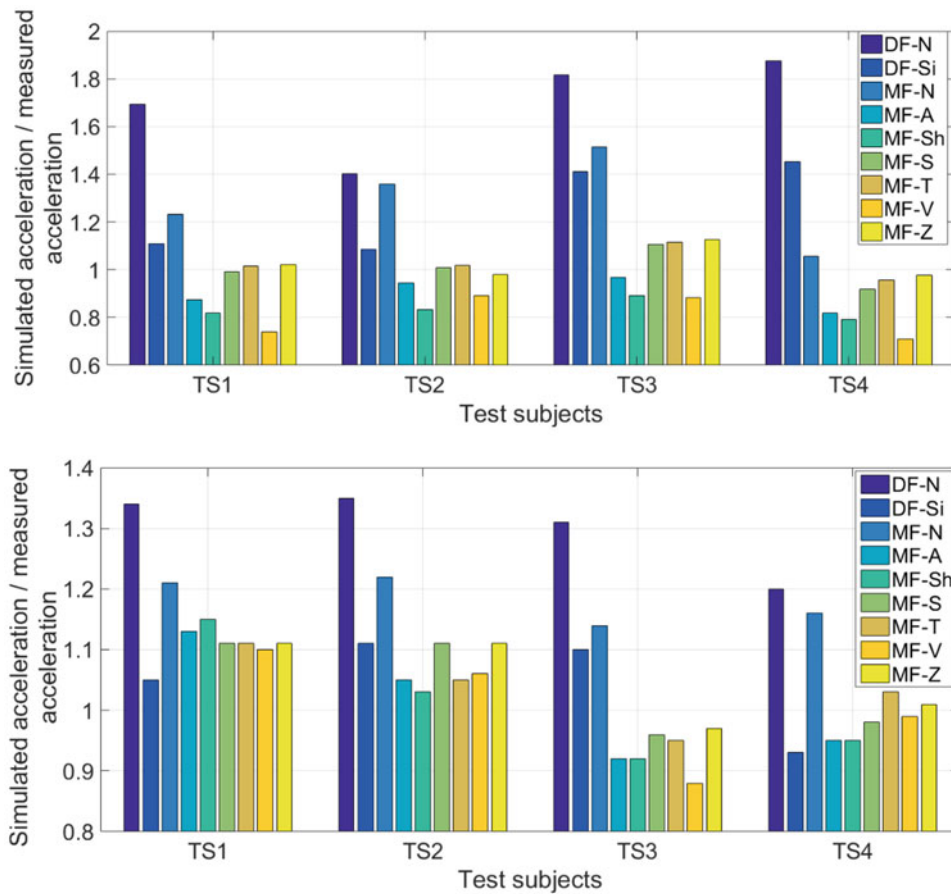


Fig. 21.5 Comparison of 1-second RMS of simulated and measured vibration responses for pacing frequencies (a) 1.9 Hz and (b) 2.05 Hz

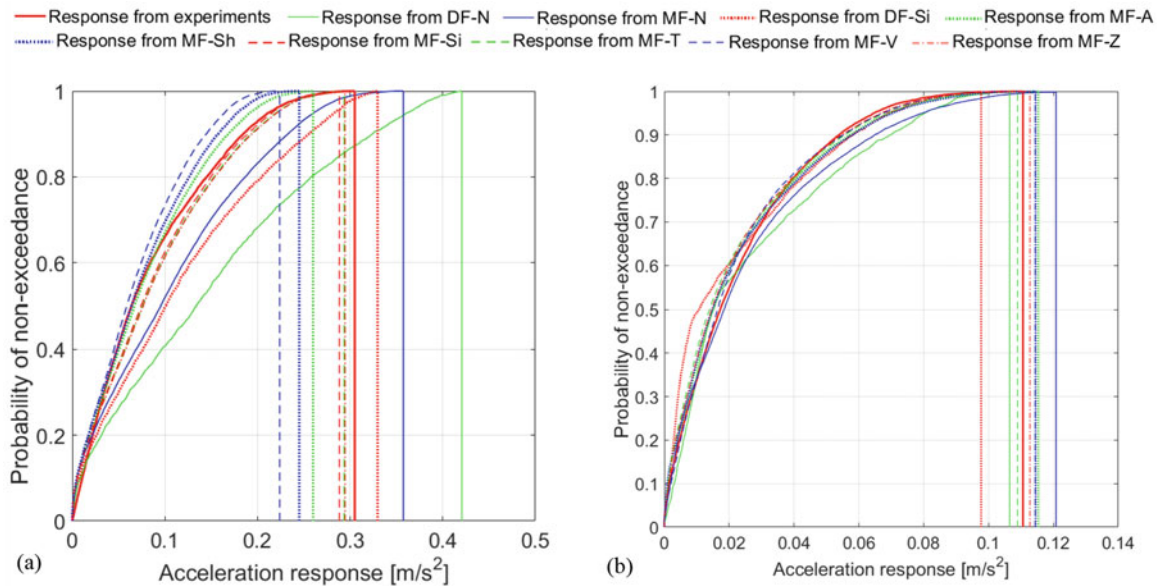
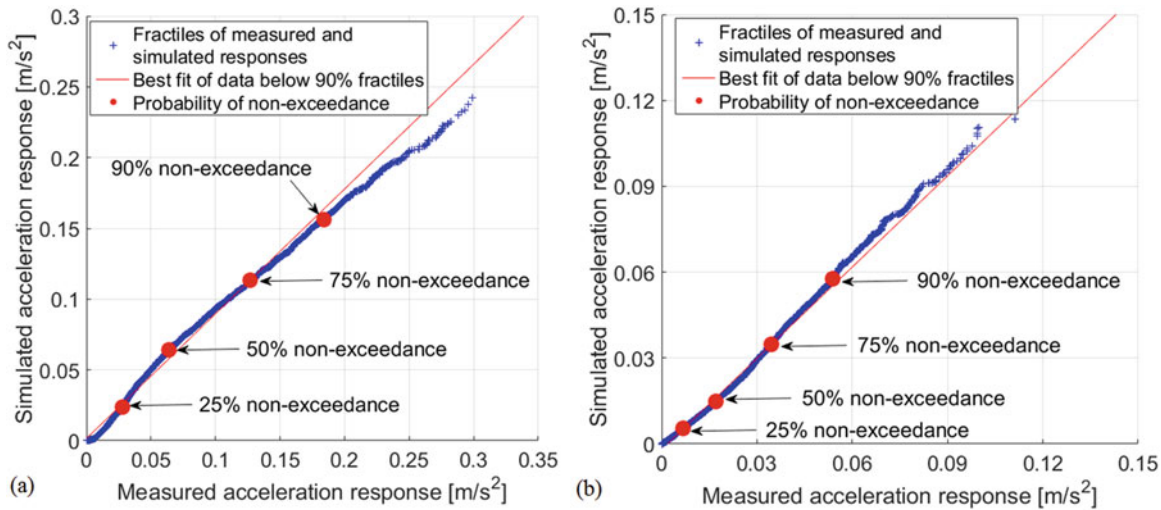


Fig. 21.6 Cumulative distribution function of vibration responses for TS1 using the model MF-Sh for pacing frequencies (a) 1.90 Hz and (b) 2.05 Hz



**Fig. 21.7** Fractiles of measured and simulated vibration responses for TS1 using MF-Sh model for pacing frequencies (a) 1.90 Hz and (b) 2.05 Hz

**Table 21.2** Average ratio of simulated/measured fractiles of vibration responses

Pacing frequency	Test subjects	Non-interactive models		Interactive models						
		Force function	Measured force	Force function	Measured force					
					Silva [8]	Alonso [6]	Shahabpoor [7]	Silva [8]	Toso [9]	Van Nimmen [10]
1.9 Hz	TS1	1.84	1.33	1.44	0.94	0.88	1.06	1.08	0.80	1.09
	TS2	1.40	1.31	1.10	0.88	0.77	0.92	0.91	0.90	0.87
	TS3	2.03	1.66	1.60	1.09	1.02	1.23	1.24	0.99	1.26
	TS4	2.08	1.17	1.62	0.89	0.88	0.96	1.03	0.78	1.06
2.05 Hz	TS1	1.29	1.20	1.08	1.06	1.06	1.02	1.03	1.01	1.01
	TS2	1.35	1.24	1.21	0.96	0.92	1.02	0.94	0.98	1.01
	TS3	1.76	1.15	1.38	0.94	0.95	0.98	0.96	0.90	0.99
	TS4	1.31	1.23	1.14	0.99	0.95	1.02	1.04	0.98	1.06
Average difference		<b>0.633</b>	<b>0.286</b>	<b>0.321</b>	<b>0.069</b>	<b>0.091</b>	<b>0.061</b>	<b>0.076</b>	<b>0.085</b>	<b>0.079</b>

Blue and red cells refer to overestimated and underestimated responses, respectively

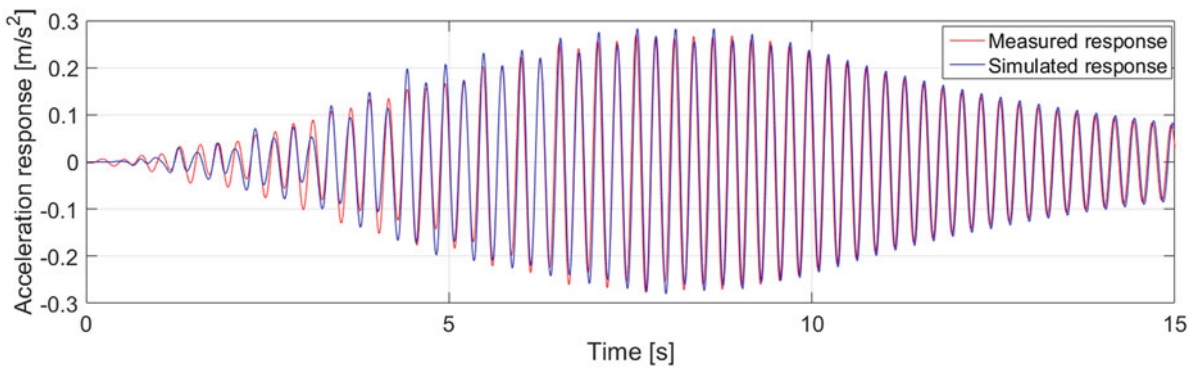


**Fig. 21.8** Measured and simulated vibration responses for TS1 using MF-Sh model for pacing frequency 1.90 Hz



## 21.5 Conclusions

This paper, compares the performance of six experimentally-developed HSI models of walking people available in the literature. The simulated vibration responses are compared with measured vibration responses pertinent to four test subjects walking on a full-scale laboratory footbridge. It is concluded that utilising any of these models can improve considerably the accuracy of the vibration responses, and some of them performed slightly better than the others. It is found also that utilising a HSI model of walking people with a reliable walking force model can produce even better accuracy.

**Acknowledgements** The authors are grateful for the College of Engineering, Mathematics and Physical Sciences in the University of Exeter for the financial support they provided for the first author and his PhD programme. The authors would also like to acknowledge the financial support provided by the UK Engineering and Physical Sciences Research Council (EPSRC) for grant reference EP/E018734/1 ('Human Walking and Running Forces: Novel Experimental Characterization and Application in Civil Engineering Dynamics').

## References

1. Zivanovic, S., Pavic, A., Reynolds, P.: Vibration serviceability of footbridges under human-induced excitation: a literature review. *J. Sound Vib.* **279**(1–2), 1–74 (2005)
2. Brownjohn, J.M.W., Racic, V., Chen, J.: Universal response spectrum procedure for predicting walking-induced floor vibration. *Mech. Syst. Signal Process.* 1–15 (2015)
3. Pavic, A., Zivanovic, S.: Key elements for probabilistic framework for estimation of structural vibration due to human-structure dynamic interaction. In: *Third International Conference on Structural Engineering, Mechanics and Computation* (2007)
4. Živanović, S.: Modelling human actions on lightweight structures: experimental and numerical developments. In: Feltrin, G. (ed.) *EVACES 2015*, p. 1005 (2015)
5. Shahabpoor, E., Pavic, A., Racic, V.: Interaction between walking humans and structures in vertical direction: a literature review. *Shock Vib.* **2016**, 12–17 (2016)
6. Jiménez-Alonso, J.F., Sáez, A.: A direct pedestrian-structure interaction model to characterize the human induced vibrations on slender footbridges. *Inf. Constr.* **66**(1), 1–9 (2014)
7. Shahabpoor, E., Pavic, A., Racic, V.: Identification of mass–spring–damper model of walking humans. *Structures*. **5**, 233–246 (2016)
8. da Silva, F.T., Pimentel, R.L.: Biodynamic walking model for vibration serviceability of footbridges in vertical direction. In: *Eurodyn 2011*, pp. 1090–1096 (2011)
9. Toso, M.A., Gomes, H.M., da Silva, F.T., Pimentel, R.L.: Experimentally fitted biodynamic models for pedestrian–structure interaction in walking situations. *Mech. Syst. Signal Process.* 1–17 (2015)
10. Van Nimmen, K., Maes, K., Živanović, S., Lombaert, G., De Roeck, G., Van den Broeck, P.: Identification and Modelling of Vertical Human-Structure Interaction, pp. 319–330. Springer, New York (2015)
11. Zhang, M., Georgakis, C.T., Qu, W., Chen, J.: SMD Model Parameters of Pedestrians for Vertical Human-Structure Interaction, pp. 311–317. Springer International Publishing, New York (2015)
12. Brownjohn, J.M.W., Fok, P., Roche, M., Omenzetter, P.: Long span steel pedestrian bridge at Singapore Changi Airport—part 2: crowd loading tests and vibration mitigation measures. *Struct. Eng.* **82**(16), 28–34 (2004)
13. Lou, J., Zhang, M., Chen, J.: Identification of Stiffness, Damping and Biological Force of SMD Model for Human Walking, pp. 331–337. Springer, New York (2015)
14. da Silva, F., Fernandes, B., Pimentel, R.: Modeling of crowd load in vertical direction using biodynamic model for pedestrians crossing footbridges. *Can. J. Civ. Eng.* **40**, 1196–1204 (2013)
15. Zivanovic, S., Pavic, A., Ingolfsson, E.T.: Modeling spatially unrestricted pedestrian traffic on footbridges. *J. Struct. Eng.* **136**, 1296–1308 (2010)